Available online at www.sciencedirect.com
ScienceDirect
Journal of the European Ceramic Society 27 (2007) 1129–1135
www.elsevier.com/locate/jeurceramsoc

Structure–properties correlations for barium titanate thin films obtained by rf-sputtering

Adelina Ianculescu [a,*], Bernard Despax [b], Vincent Bley [b], Thierry Lebey [b], Raluca Gavrilă [c], Nicolae Drăgan [d]

[a] *Department of Oxide Materials Science and Engineering, "Politehnica" University of Bucharest, 1-7 Gh. Polizu, P.O. Box 12-134, 011061 Bucharest, Romania*
[b] *Laboratory of Electrical Engineering, Paul Sabatier University, 118 Route de Narbonne, F31062 Toulouse, France*
[c] *National Institute for Research and Development in Microtechnologies, 32B Erou Iancu Nicolae, P.O. Box 38-160, 77225 Bucharest, Romania*
[d] *Institute of Physical Chemistry "I.G. Murgulescu" of the Romanian Academy, 202 Splaiul Independentei, 060021 Bucharest, Romania*

Available online 12 June 2006

Abstract

Stoichiometric thin films were deposited by rf-magnetron sputtering from a $BaTiO_3$ ceramic target on Pd foils used as substrates. Polycrystalline $BaTiO_3$ films with different grain sizes were obtained by post-deposition heat treatment in air, at 900 °C for 8 h. A multi-step deposition–annealing technique was used in order to improve the compactness and therefore, the dielectric behaviour.

The structural characteristics and the surface topography varied obviously with both films thickness and deposition–annealing procedure. X-ray diffraction data pointed out that the so-called "pseudocubic" phase, generally reported for such fine-grained thin films, does not involve only a highly distorted unit cell, but consists obviously, in our case, from a mixture of crystalline phases, with tetragonal and cubic symmetry, respectively.

The dielectric properties (relative permittivity and loss tangent) showed small frequency dispersion. The $BaTiO_3$ film of 0.6 μm thickness obtained by four deposition–annealing cycles exhibited a dielectric constant of ~700 and a dissipation factor of 0.06 at 100 kHz.

Keywords: Films; Grain size; X-ray methods; Dielectric properties; $BaTiO_3$

1. Introduction

Barium titanate is one of the most widely studied ferroelectric materials due to its many potential useful properties. Particularly, $BaTiO_3$-based thin films have received much attention in recent years for their numerous applications in microelectronics and integrated optics technologies, ranging from buffer layers for the integration of high-temperature superconductors and voltage-tunable microwave filters, to pyroelectric imaging arrays and multifunctional highly integrated CMOS-based devices, such as nonvolatile random access memories (NVRAM) and dynamic random access memories (DRAM).[1–4] Thin film ferroelectric devices offer several advantages over their bulk counterparts, such as lower driving voltages, higher speed and the potential for monolithic integration with Si.

Beside the large variation in the reported values of the thin films dielectric permittivity caused by the different deposition techniques and processing parameters used, other problems concerning deviations of structural and electrical properties from those of bulk ceramics have been noticed. Thus, many authors[5–7] pointed out the so-called "crystal size effect", which determines diffuse ferroelectric–paraelectric phase transition in fine-grained $BaTiO_3$ films, irrespective of the processing route. In an attempt to understand the electrical behaviour, we carried out earlier[8] a structural analysis of such fine-grained $BaTiO_3$ thin films deposited by rf-sputtering.

Taking into account that a major barrier in the widespread use of these films in a number of high-frequency applications is their high leakage currents determined by structural defects as grain boundaries and oxygen vacancies, several approaches including the introducing of intermediate oxygen relaxation or of thin epitaxial intermediate layers were also proposed.[9]

In this work, we try to emphasize the influence of both thickness and deposition–annealing procedure on the structure of the $BaTiO_3$ films and to correlate these structural parameters with

* Corresponding author. Tel.: +40 21 4023848; fax: +40 21 3181010.
E-mail address: a.ianculescu@rdslink.ro (A. Ianculescu).

0955-2219/$ – see front matter © 2006 Elsevier Ltd. All rights reserved.
doi:10.1016/j.jeurceramsoc.2006.05.043

the dielectric properties. We proposed here a multi-step deposition technique, in order to improve the dielectric behaviour, especially from the point of view of both dielectric losses and tunability.

2. Experimental

2.1. Samples preparation

$BaTiO_3$ thin films of 0.6 and 1 μm thicknesses were deposited by rf-magnetron sputtering technique from a hot pressed $BaTiO_3$ ceramic target onto Pd foils used as substrates. The sputtering atmosphere was pure argon maintained at pressures ranged between 0.4 and 1 Pa. The substrate holder was heated to a temperature of 300 °C. Under the above conditions, the deposition rate was more important in the central part of the discharge (∼18 nm/min) and decreased gradually to the periphery (∼5 nm/min). We found that the films deposited on the substrates placed at the edge of the samples holder (6 cm on the radial axis) are of better quality from chemical point of view, showing no significant off-stoichiometry Ba/Ti ratios (Table 1). The as-grown films were amorphous. Post-deposition annealing of the samples was carried out in air to obtain crystalline films.

A four-step deposition–annealing technique was also developed in order to improve the $BaTiO_3$ structure and compactness and therefore, to reduce the dielectric losses. To compare the influence of both thickness and deposition–annealing procedure on the films properties, we analyzed three different $BaTiO_3$ samples: two single-deposit films (of 0.6 and 1 μm, respectively) obtained by annealing in air, with a heating rate of 5 °C/min up to 900 °C, with 8 h plateau at this temperature and a $BaTiO_3$ film of 0.6 μm, with four successive deposits, followed each of them by an annealing in the same conditions (again 900 °C/8 h, in air). After each thermal treatment, the samples were slowly cooled to room temperature with a cooling rate of 1.5 °C/min.

2.2. Samples characterization

The Ba/Ti ratio was measured by means of X-ray fluorescence spectroscopy using a Tracor X-ray Spectrance 5000 equipment.

In order to establish the phase composition, X-ray diffraction analyses were carried out with a Shimadzu XRD 600 diffractometer using Ni-filtered Cu Kα radiation with scan step increments of 0.02° and with a counting time of 1 s/step, for 2θ ranged between 20° and 80°. To estimate the structural characteristics (unit cell parameters, crystallite average size and orientation degree) the same step increment but with a counting time of 10 s/step, for 2θ ranged between 20° and 120° was used. Parameters to define the position, magnitude, shape and integral breadth or full width at half maximum of profile (FWHM) of the individual peaks are obtained using the pattern fitting and profile analysis of the original X-ray 3.0 program. The lattice constants calculation is based on the least squares procedure (LSP) using the linear multiple regressions for several XRD lines, depending

Table 1
Chemical composition and structural characteristics of the analyzed films

Characteristics	Target	Sample 1	Sample 2	Sample 3
No. of deposits	–	1	4	1
Film thickness (μm)	–	0.6	0.6	1
Ba/Ti ratio	1.002 ± 0.002	0.985 ± 0.005	0.995 ± 0.003	0.998 ± 0.003
Unit cell parameters (Å)				
Cubic				
a	–	4.0300 ± 0.0123	4.0131 ± 0.0103	4.0270 ± 0.0089
Tetragonal				
c	4.0100 ± 0.0033	4.0369 ± 0.0089	4.0268 ± 0.0063	4.0244 ± 0.0034
a	3.8969 ± 0.0023	3.9943 ± 0.0064	3.9987 ± 0.0044	3.9988 ± 0.0023
Tetragonality, *c*/*a*	1.029	1.011	1.007	1.006
Unit cell volume, V (Å^3)				
Cubic	–	65.45 ± 0.60	64.63 ± 0.50	65.31 ± 0.43
Tetragonal	63.74 ± 0.13	64.41 ± 0.35	64.39 ± 0.24	64.37 ± 0.13
Average crystallite size, $\langle D \rangle$ (Å)				
Cubic	–	583	1174	600
Tetragonal	938	568	779	686
Internal strain, $\langle S \rangle \times 10^3$				
Cubic	–	0.7	0.9	0.5
Tetragonal	0.6	0.6	0.5	0.2
(1 1 1) orientation degree, α_{111}				
Cubic	–	0.376 ± 0.017	0.394 ± 0.021	0.258 ± 0.014
Tetragonal	0.224 ± 0.013	0.486 ± 0.018	0.431 ± 0.020	0.439 ± 0.018
(2 0 0) orientation degree, α_{200}				
Cubic	–	0.368 ± 0.017	0.429 ± 0.020	0.364 ± 0.016
Tetragonal	0.249 ± 0.012	0.495 ± 0.019	0.295 ± 0.016	0.462 ± 0.017

on the unit cell symmetry. To deconvolute size, D, and strain, S, broadening from the XRD spectra, the multiple line analysis and integral breadth methods applied to the observed profiles (properly approximated with the Pearson's VII analytic functions) were used.

AFM measurements were effected in order to determine the surface roughness and to estimate the surface topography.

To perform the electrical measurements, gold dots of 1 mm diameter and of 75 nm thickness were sputtered as top electrodes through a mask onto the surface of crystalline $BaTiO_3$ films. The Pd substrate was used as bottom electrode. Capacitance and dielectric losses were measured by using a Hewlett Packard 4284 A LCR-meter from 80 Hz to 1 MHz frequency range. Temperature dependence of the dielectric constant was measured by placing samples in a small oven and heating them in air. The bias dependence of the capacitance was investigated to determine the ferroelectric state of the films. A 1 V signal was used to measure the capacitance at 100 kHz as the bias voltage was ramped between −10 and +10 V.

3. Results and discussions

3.1. Structural characteristics

The X-ray diffraction patterns of the three samples analyzed here show the presence of well-crystallized $BaTiO_3$ (Fig. 1). No Ti- or Ba-rich secondary phases were detected in the annealed films.

The main peaks of the palladium substrate, as well as of PdO formed because of Pd oxidation during the annealing were also detected. We found that all the samples consist of two $BaTiO_3$ forms: one with cubic symmetry and the other with tetragonal symmetry. The cubic phase was identified on the diffractograms

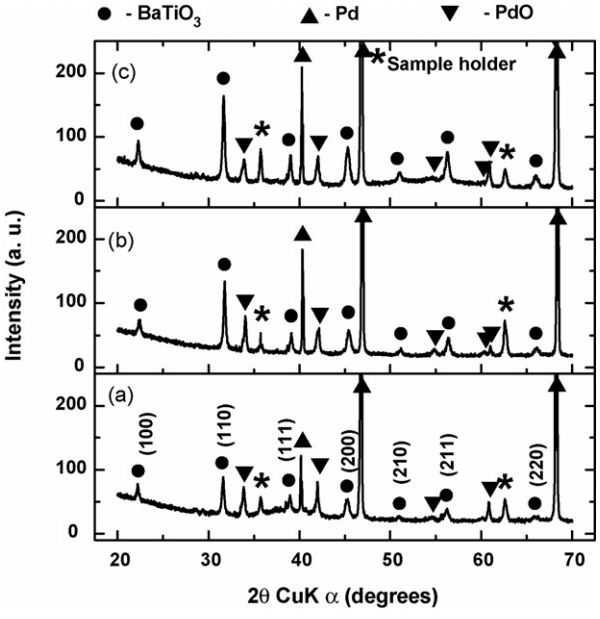

Fig. 1. X-ray diffractions patterns for the analyzed samples: (a) one-deposit film of 0.6 μm thickness, (b) four-deposit film of 0.6 μm thickness and (c) one-deposit film of 1 μm thickness.

as small shoulders placed at the left side ($2\theta = 38.4$–38.7° and 44.7–44.8°) of both (1 1 1) and (2 0 0) peaks (JCPDS-file no. 75-214). The thinner the films, the more visible were these shoulders.

The structural characteristics of both thin films and ceramic target (used as standard sample) were summarized in Table 1.

First of all, we assumed that the four-deposit film (sample 2) is heterogeneous from the point of view of crystallite size. It is probable that the internal layers, subjected to successive annealings, consist of larger crystallites, than the smaller ones of the surface layer. The plateau of the cumulative annealings increases from only 8 h, for the last deposit to 32 h for the first one. This assumption was sustained by average crystallite size values, which indicated the obtaining of larger crystallites for thicker films (sample 3) and, especially, for multi-layer films (sample 2). For thin films the average crystallite size values have to be correlated with these ones of internal strains. It is well known fact that the internal strains increase as the average crystallite size decreases. Thus, it is not surprising that weaker internal strains were determined for the thicker film (sample 3). Concerning the multi-layer thin film, the cubic phase seems to be more stressed than the tetragonal one, despite its crystallinity. In this case, additional internal strains between the different layers cannot be excluded.

Higher values of unit cell parameters for tetragonal $BaTiO_3$ form in thin films were obtained in comparison with those of the bulk ceramic target. The crystallinity increase, due to either the thickness increasing or to the successive annealings, involves no-significant increase of a but more pronounced decrease of c, so that the tetragonality was slightly affected. Anyway, low tetragonality values were obtained, because of the strongly distorted perovskite lattice. Because of the concurrent evolution of the two parameters against the average crystallite size, the shrinkage of the tetragonal unit cell is very small, its volume being nearly constant. The shrinkage was more obvious for the cubic form, whose unit cell parameter decreases with the films crystallinity.

Comparing with the ceramic target, all the films analyzed exhibit preferential [1 1 1] and [2 0 0] orientations.

The orientation degree named α_{hkl} was calculated using Eqs. (1) and (2):

$$\alpha_{hkl} = \frac{I_{hkl}}{I_{hkl} + I_{110}} \tag{1}$$

$$I^{\text{calc}}_{hkl} = I^{\text{calc}}_{\text{max}} - I_{\text{background}}, \tag{2}$$

where I^{calc}_{hkl} represents the calculated integrated intensity of the (hkl) peak obtained after the subtraction of the background intensity, $I_{\text{background}}$, from the maximal integrated intensity $I^{\text{calc}}_{\text{max}}$ of the same peak.

Some aspects have to be emphasized:

(i) For one-deposit samples the orientation degree along the two directions mentioned was higher (compared to the one corresponding to the bulk target) as the film thickness was lower; unlike the tetragonal phase, where a preferential orientation between the two crystallographic directions is not

very obvious, the cubic form clearly exhibits a preferential [1 1 1] orientation.

(ii) For samples with similar thickness, the greater the number of deposits, the more favourable seems to be a random orientation of the tetragonal form, close to that of bulk ceramics; the decrease of the orientation degree is more visible for [2 0 0] direction; a contrary tendency, of preferential [2 0 0] orientation was pointed out for the cubic form in this multilayer sample.

3.2. Surface topography

The AFM topography of the three samples was presented in Fig. 2(a–c). Fig. 2(a) shows the topography of a one-deposit film (sample 1), which presents a RMS surface roughness of 37.9 nm. One can notice well-defined grain-boundaries having between them a great number of small dark zones, which represent valleys (holes, pits) uniformly distributed on the film surface. These films seem to be not very smooth, taking into account the roughness value.

The situation completely changes for the four-deposit film (sample 2). In this case, the film surface looks more "furrowed". In comparison with the "one-layer" sample, there are only a few very large, non-uniform (as shape and size) and randomly distributed "depression" zones.

In order to distinguish the surface roughness from the superimposed surface waviness present on the micrometer length scale, a high-pass Fourier filtering was performed on the overall profile height. The result is displayed in Fig. 2(c). In these conditions a decreased surface roughness (RMS = 22.9 nm), higher densification and smaller grains than the ones corresponding to the one-layer sample were noticed. These observations apparently do not match the XRD results related to the average crystallite size, which pointed out larger crystallites in the four-deposit film. The results are however plausible, if we take into account the fact that in AFM images only the grains surface is observed and if we assume the heterogeneity of the crystallite size across the film thickness (because of the increased annealing time endured by each successive layer). In order to elucidate this aspect supplementary cross-section TEM analyses are required. The "furrowed" surface, as well as the presence of finer grains in the surface layer of sample 2 suggests that the interface between the last two deposits may act as an active, discontinuous nucleation surface for the fourth layer crystallization. In other words, the nucleation process is more favourable than the crystals growth, at least for the crystallization of the last deposit of this film.

3.3. Dielectric behaviour

The frequency response in all the films analyzed here shows a power law dependence specific to highly disordered structures (Fig. 3(a–c)) and obviously different from the pure Debye resonances displayed by the bulk $BaTiO_3$. This behaviour has been

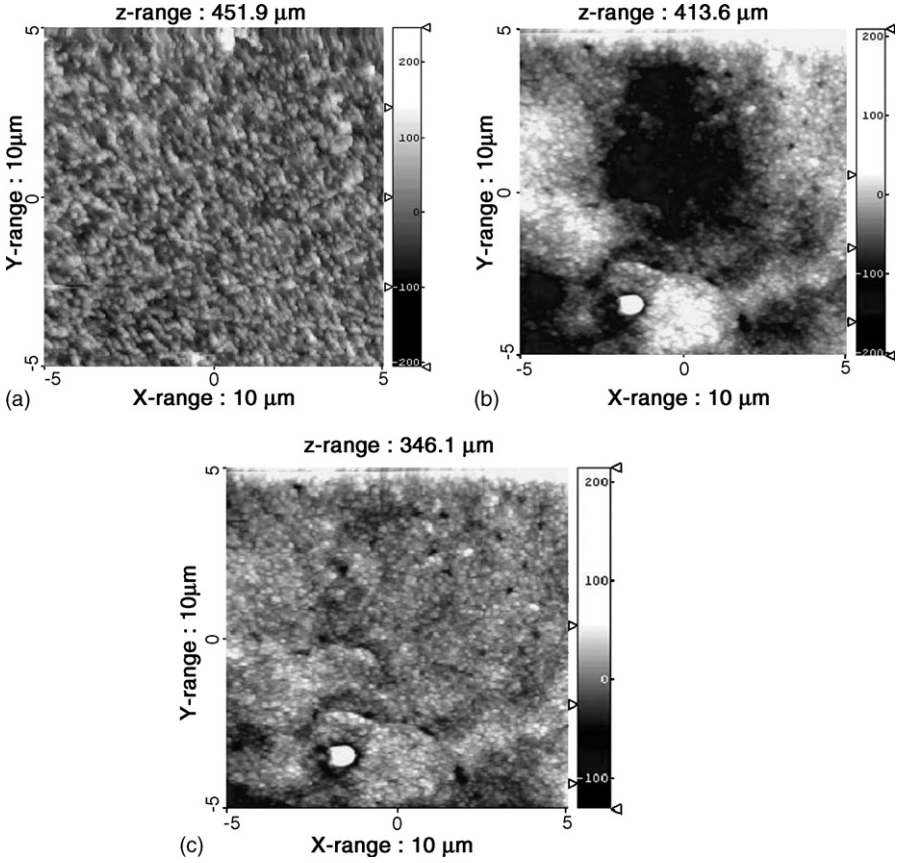

Fig. 2. AFM images of: (a) sample 1, (b) non-filtered sample 2 and (c) filtered sample 2.

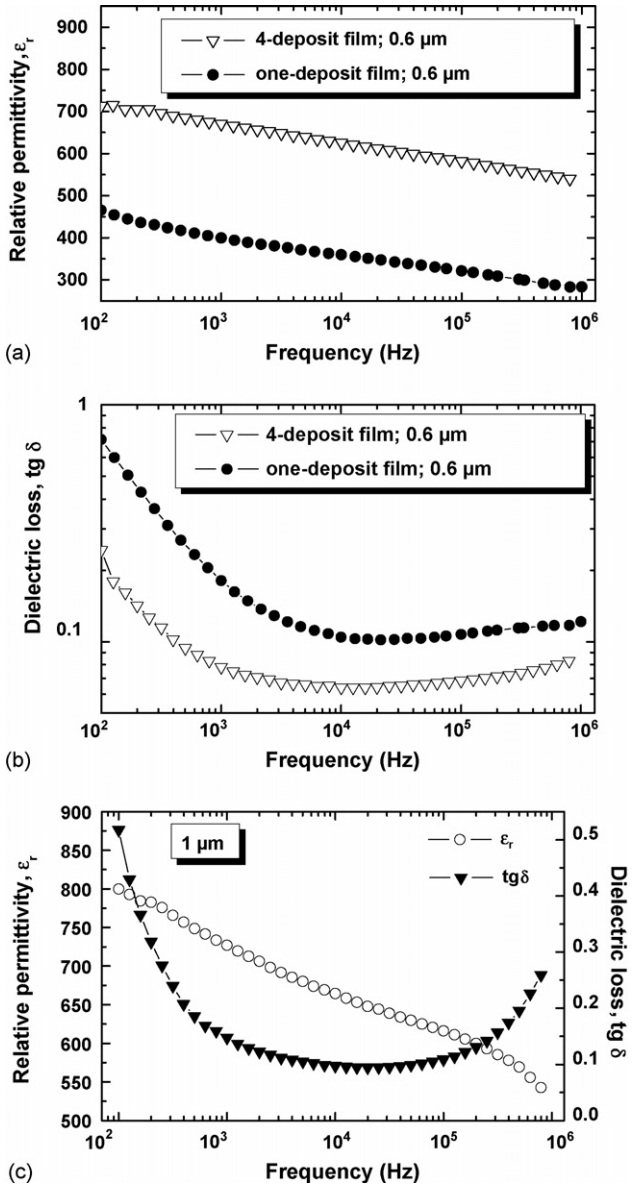

Fig. 3. Frequency response of the dielectric properties measured at room temperature, in the $BaTiO_3$ thin films analyzed: (a) relative permittivity evolution for samples 1 and 2, respectively, (b) dielectric loss evolution for samples 1 and 2, respectively, and (c) relative permittivity and dielectric loss for sample 3.

attributed to inhomogeneities resulting from either the presence of boundaries or point defects, which modify the local charge density.[5]

For the one-deposit samples, concurrent high dielectric losses (of $1–5 \times 10^{-1}$), especially in the lower frequencies range were also recorded (Fig. 3(b and c)). As already mentioned, the thinner films consist of smaller grains. The smaller the average grain size, the smaller the grain-to-boundary ratio, which determines a lower overall permittivity of the film, as well as higher dielectric losses because of the higher leakage currents. These observations are in good agreement with those reported by Shaw et al.[6] and Hayashi et al.[10]

Concerning the four-deposit film, due to its more dense microstructure and higher overall crystallite size, higher permittivity and significantly lower dielectric losses were obtained (Fig. 3(a and b)). For frequencies ranged between 10^3 and 10^5 Hz, the dielectric loss shows values of 0.06–0.07, comparable with those ones specific to $BaTiO_3$ bulk ceramics. Even though this multi-layer film is thinner (0.6 μm), due to its higher crystallinity, its dielectric constant approaches the permittivity value of the thicker (1 μm) one-deposit film.

Fig. 4(a–c) shows the temperature dependence of the relative permittivity, at different frequency values for $BaTiO_3$ thin films studied here. Diffuse phase transitions, with no typical anomaly around 120 °C related in bulk $BaTiO_3$ to the transformations from tetragonal (ferroelectric) to cubic (paraelectric) phase were noticed. For single-deposit films (Fig. 4(a and c)) almost constant variations of the dielectric constant against the temperature were observed up to 90–100 °C, followed by linear decreasing

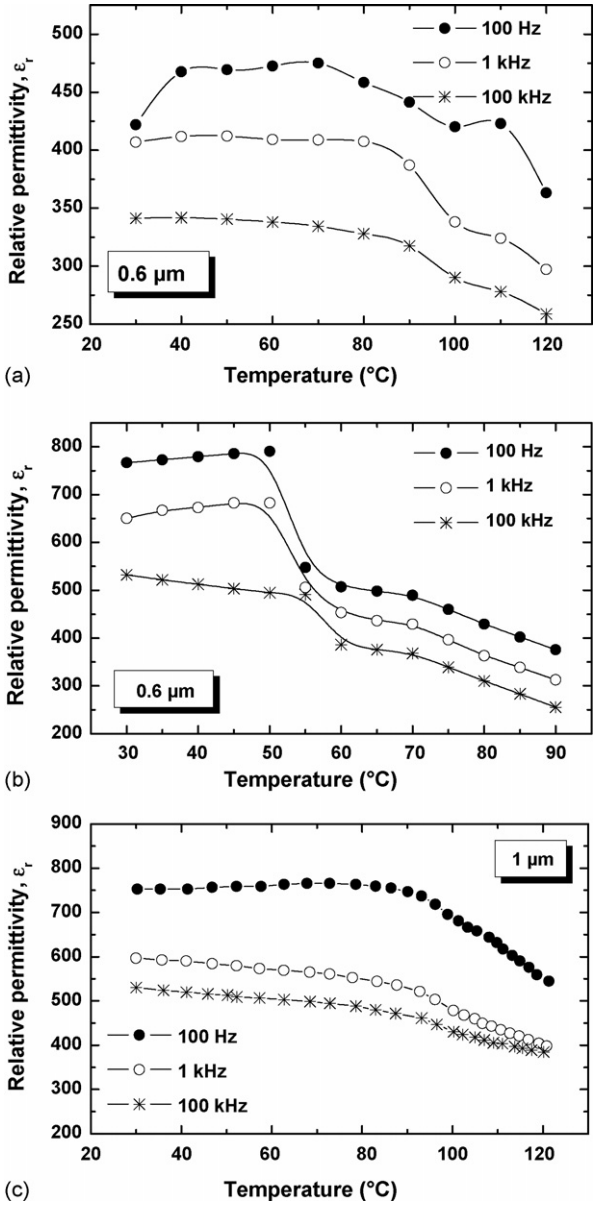

Fig. 4. Temperature dependence of dielectric constant, ε_r of: (a) sample 1, (b) sample 2 and (c) sample 3.

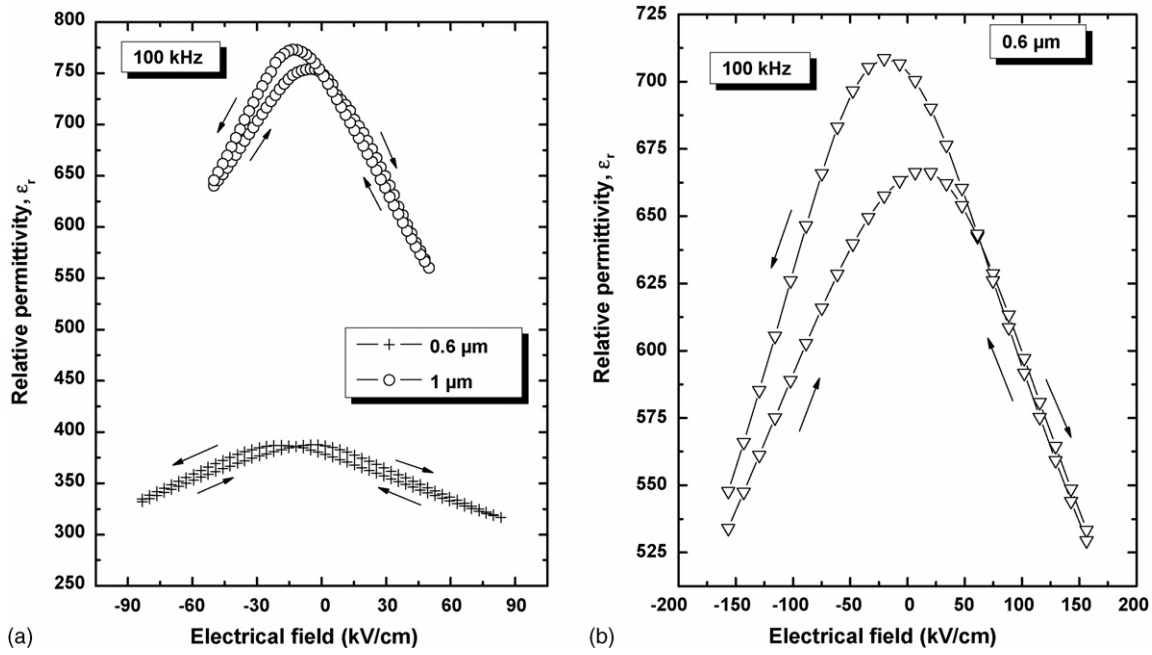

Fig. 5. Relative permittivity–electrical field characteristics at room temperature and at 100 kHz frequency of: (a) single-deposit films (samples 1 and 3) and (b) four-deposit film (sample 2).

of this property at higher temperature. We consider that this phenomenon is a consequence of the highly distorted structure, consisting of two different $BaTiO_3$ forms. Even the tetragonal phase was certainly identified, the strong internal strains, the stress induced by the substrate, as well as the domains pinning due to the fine grains, essentially contribute to this behaviour. Similar results were obtained by Hayashi et al.[10] for their thin films prepared by sol–gel method. On the other hand, our results differ from those reported by Dharmadhikari and Granneman[11] and Norton et al.,[12] which showed broad peaks in ε_r–T characteristic around 120 °C for their rf-sputtered and pulsed-laser deposited thin films.

Sharper dependence was observed, especially at lower frequencies, for the four-deposit film, probably due to the larger crystallites, as the X-ray diffraction analyses pointed out (Fig. 4(b)).

The variation in the dielectric response with the dc bias is associated with the domain reorientation process.[13] Fig. 5(a and b) shows the field-dependent dielectric permittivity of $BaTiO_3$ films measured at 100 kHz. A typical hysteresis between the ε_r–E plots specific to the up- and down-ramped dc bias was recorded for all samples, indicated the non-linear nature of these films (Fig. 5(a and b)).

It is well-known that the shape of the ε_r–E characteristic is indicative of the domains distribution. It can be seen from Fig. 5(a) that a single-layer thick film (sample 3) exhibits a more sharply humped ε_r–E characteristic in comparison with that one of a thinner film (sample 1). This effect is obvious also for the four-deposit film (Fig. 5(b)). Supplementary measurements revealed that the integrity of this multi-layer film is maintained, even as the electrical field varied between −300 and +300 kV/cm.

The tunability of the films was calculated according to the following formula:[14]

$$\text{tunability}\,(\%) = \frac{\varepsilon_{max} - \varepsilon_{min}}{\varepsilon_{max}} \times 100, \quad (3)$$

where ε_{max} and ε_{min} are the maximum and the minimum relative permittivities.

It is worthy to notice that the tunability is directly related to the dielectric permittivity of the materials, so that a higher dielectric constant will result in a higher tunability.[15] Therefore, we concluded that higher crystallinity involves also higher tunability. For this reason, referring to single-deposit samples, the thicker film (of 1 μm) exhibits higher tunability than the thinner one (of 0.6 μm). Thus, for an electrical field of 50 kV/cm, sample 3 displayed a tunability of ∼27% in comparison with the tunability of only ∼11% obtained for sample 1.

Higher densification and crystallinity of the multi-deposit specimen (sample 2) lead not only to a higher dielectric constant value, but also to a more intense electrical field which can be supported by this film, comparing to single-deposit film (sample 1) of the same thickness (0.6 μm). A tunability of ∼26% for an electrical field of 160 kV/cm was obtained for this four-deposit $BaTiO_3$ film.

4. Conclusions

A multi-step deposition–annealing technique was proposed in order to improve the compactness and therefore, the dielectric behaviour. X-ray diffraction data pointed out that the $BaTiO_3$ thin films studied consist of a mixture of crystalline forms, with tetragonal and cubic symmetry, irrespective of the thickness or processing technique. A lower surface roughness (∼23 nm) was

estimated for the four-deposit film, in comparison to that one specific to the one-deposit film (∼39 nm) with the same thickness.

The dielectric properties were correlated with the structural parameters, especially by means of average crystallite size. The multi-layer $BaTiO_3$ film shows higher crystallinity degree and higher densification, so that higher relative permittivity and lower dielectric losses were obtained in this case, in comparison with the single-deposit film with similar thickness. Thus, the film of 0.6 μm obtained by four deposition–annealing cycles exhibits a dielectric permittivity of ∼700 and a dissipation factor of 0.06 at 100 kHz.

References

1. Scott, J. F., Device physics of ferroelectric thin-film memories. *Jpn. J. Appl. Phys.*, 1999, **38**, 2272–2274.
2. Ramesh, R., Aggarwal, S. and Auciello, O., Science and technology of ferroelectric films and heterostructures for non-volatile ferroelectric memories. *Mater. Sci. Eng.*, 2001, **32**, 191–236.
3. Rose, T. L., Kelliher, E. M., Scoville, A. N. and Stone, S. E., Characterization of rf sputtered $BaTiO_3$ thin films using a liquid electrolyte. *J. Appl. Phys.*, 1984, **55**, 3706–3714.
4. Kuroiwa, T., Tsunemine, Y., Horikawa, T., Makita, T., Tanimura, J., Mikami, N. *et al.*, Dielectric properties of $(Ba_xSr_{1-x})TiO_3$ thin films prepared by rf sputtering for dynamic random access memory application. *Jpn. J. Appl. Phys.*, 1994, **33**, 5187–5191.
5. Hoeman, B. H., Ford, G. M., Kaufmann, L. D. and Wessels, B. W., Dielectric properties of epitaxial $BaTiO_3$ thin films. *Appl. Phys. Lett.*, 1998, **73**, 2248–2250.
6. Shaw, T. M., Suo, Z., Huang, M., Liniger, E., Laibowitz, R. B. and Baniecki, J. D., The effect of stress on the dielectric properties of barium strontium titanate thin films. *Appl. Phys. Lett.*, 1999, **75**, 2129–2131.
7. Sharma, B. H., Sarma, H. N. K. and Mansingh, A., Fatigue in sol–gel derived barium titanate films. *J. Appl. Phys.*, 1999, **85**, 341–346.
8. Preda, L., Despax, B., Courselle, L., Bandet, J. and Ianculescu, A., Structural characteristics of rf-sputtered $BaTiO_3$ thin films. *Thin Solid Films*, 2001, **389**, 43–50.
9. Petrov, P. Kr., Carlsson, E. F., Larsson, P., Friesel, M. and Ivanov, Z. G., Improved $SrTiO_3$ multilayers for microwave application: growth and properties. *J. Appl. Phys.*, 1998, **84**, 3134–3140.
10. Hayashi, T., Oji, N. and Maiwa, H., Film thickness dependence of dielectric properties of $BaTiO_3$ thin films prepared by the sol–gel method. *J. Appl. Phys.*, 1994, **33**, 5277–5280.
11. Dharmadhikari, V. S. and Granneman, W. W., Photovoltaic properties of ferroelectric $BaTiO_3$ thin films rf-sputter deposited on silicon. *J. Appl. Phys.*, 1982, **53**, 8988–8992.
12. Norton, M. G., Cracknell, K. P. B. and Carter, B., Pulsed-laser deposition of barium titanate thin films. *J. Am. Ceram. Soc.*, 1992, **75**, 1999–2002.
13. Lines, M. E. and Glass, A. M., *Principles and Applications of Ferroelectric and Related Materials*. Clarendon, Oxford, 1977, pp. 133–139.
14. Im, J., Auciello, O., Baumann, P. K., Streiffer, S. K., Kaufman, D. Y. and Krauss, A. R., Composition-control of magnetron-sputter-deposited $(Ba_xSr_{1-x})Ti_{1+y}O_{3+z}$ thin films for voltage tunable devices. *Appl. Phys. Lett.*, 2000, **76**, 625–627.
15. Sengupta, L. C. and Drach, W. C., Investigation of the electronic properties of doped $Ba_{1-x}Sr_xTiO_3$ phase shifting materials. *Ferroelectrics*, 1994, **153**, 359–364.